PROTEINS: Structure, Function, and Genetics 48:283–292 (2002)

The Role of Hydrophobic Microenvironments in Modulating pK_a Shifts in Proteins

E.L. Mehler,[1]* M. Fuxreiter,[2] I. Simon,[2] and B. Garcia-Moreno E[3]
[1] *Department of Physiology and Biophysics, Mount Sinai School of Medicine, New York, New York*
[2] *Institute of Enzymology, Hungarian Academy of Sciences, Budapest, Karolina ut 29, Hungary*
[3] *Department of Biophysics, Johns Hopkins University, Baltimore, Maryland*

ABSTRACT **The screened Coulomb potential (SCP) method, combined with a quantitative description of the microenvironments around titratable groups, based on the Hydrophobic Fragmental Constants developed by Rekker, has been applied to calculate the pK_a values of groups embedded in extremely hydrophobic microenvironments in proteins. This type of microenvironment is not common; but constitutes a small class, where the protein's architecture has evolved to lend special properties to the embedded residue. They are of significant interest because they are frequently important in catalysis and in proton and electron transfer reactions. In the SCP treatment these special cases are treated locally and therefore do not affect the accuracy of the pK_a values calculated for other residues in less hydrophobic environments. Here the calibration of the algorithm is extended with the help of earlier results from lysozyme and of three mutants of staphylococcal nuclease (SNase) that were specially designed to measure the energetics of ionization of titratable groups buried in extremely hydrophobic microenvironments. The calibrated algorithm was subsequently applied to a fourth mutant of SNase and then to a very large dimeric amine oxidase of 1284 residues, where 334 are titratable. The observed pK_a shifts of the buried residues are large (up to 4.7 pK units), and all cases are well reproduced by the calculations with a root mean square error of 0.22. These results support the hypothesis that protein electrostatics can only be described correctly and self-consistently if the inherent heterogeneity of these systems is properly accounted for. Proteins 2002;48:283–292.**

Key words: pKa in proteins; protein electrostatics; hydrophobicity of microenvironments; pK_a and hydrophobicity; solvation

INTRODUCTION

It is well established that titratable residues (TRs) often play key roles in enzyme catalysis by their involvement in proton transfer processes. To facilitate these processes, proteins evolve special environments surrounding the functionally active groups, which can lead to very large shifts in pK_a values.[1–8] Large shifts in pK_a values have also been observed in proteins involved in electron transport[9–12] and in cases where a TR does not play a direct functional role, which might represent an adaptation to ensure that the residue remain in a particular charge state[13,14] regardless of the fluctuations in local pH. They have also been observed recently in artificial cases, where TRs were buried in the hydrophobic core of a protein by mutagenesis, precisely to test the properties of TRs in these environments.[15,16]

Considerable progress has been made in the last several years in the calculation of pK_a values of TRs in proteins. The overall reliability of the calculations is quite reasonable. Nevertheless, most methods still have considerable difficulty reproducing very large pK_a shifts with acceptable accuracy.[17] One reason for this is that most approaches treat the protein as a homogeneous medium, although it is generally accepted that proteins are extremely anisotropic and heterogeneous.[18] Moreover, because the protein effects large pK_a shifts by creating local environments with special properties that can deviate greatly from the average, treating the system homogeneously practically precludes the ability to calculate such large shifts. The assumption of homogeneity is expressed by using a single screening parameter to describe the entire protein, i.e., the so-called internal dielectric constant, although it has little meaning in a microscopic system. These matters have been discussed thoroughly by Warshel and collaborators, who have consistently pointed out that the screening parameter cannot be constant but

September 11, 2001: This article is dedicated to all those who lost their lives in the inferno of hatred that destroyed the WTC and struck the Pentagon, and to the passengers and crew of United Flight 93 who leave behind a few pictures and memories in the minds and hearts of those who loved them.

The program for performing pKa calculations of the type discussed in this paper is available. Contact the corresponding author at mehler@inka.mssm.edu or go to URL: http://fulcrum.physbio.mssm.edu/~mehler/text/pka.html, for further information.

Grant sponsor: National Institutes of Health; Grant number: NIDA # DA15170 (ELM); Grant sponsor: National Institutes of Health; Grant number: GM # 61597 (BG-ME); Grant sponsor: OTKA; Grant number: D34572 (MF); Grant sponsor: Bolyai fellowships (MF); Grant sponsor: OKTA grants; Grant numbers: project numbers T30566, T34131.

*Correspondence to: E.L. Mehler, Mount Sinai School of Medicine, Department of Physiology and Biophysics, New York, NY 10029. E-mail: mehler@inka.mssm.edu

Received 15 October 2001; Accepted 7 March 2002

depends on the thermodynamic quantity that is being calculated as well as on the specific model employed for the calculations.[17,19–23] It has also been shown that at least for interactions between charged groups, the screening is always large, even when both charged groups are well buried in the protein.[19] These observation are based on a large number of pK_a calculations reported in the literature and on the properties of ionizable residues observed experimentally.[15–17,24,25]

In proteins pK_a values are calculated relative to a reference state. The procedure is based on the following thermodynamic cycle[26,27]:

$$\begin{array}{ccc} & 2.303RT\mathrm{p}K_a^A(s) & \\ AH(s) & \Leftrightarrow & A^-(s) + H^+(s) \\ \Uparrow & & \Uparrow \\ \Delta\mu_{s,p}(AH) & & \Delta\mu_{s,p}(A^-) \\ \Downarrow & & \Downarrow \\ AH(p) & \Leftrightarrow & A^-(p) + H^+(s) \\ & 2.303RT\mathrm{p}K_a^A(p) & \end{array} \qquad (1)$$

where p$K_a^A(s)$ is the reference value of titratable group A, and p$K_a^A(p)$ is the value in the protein. The $\Delta\mu$ are the chemical potentials of transfer between the solvent and the protein. Considering only the electrostatic contributions, p$K_a^A(p)$ is calculated from

$$\mathrm{p}K_a^A(p) = \mathrm{p}K_a^A(s) + (w_A^{\mathrm{int}} + \alpha_A \Delta w_A^{\mathrm{tr}})/2.303RT \qquad (2)$$

where w_A^{int} is the interaction electrostatic free energy of the charged group in the field of all the other groups in the protein, Δw_A^{tr} is the change in self-energy on transferring the group from water into the protein and α_A is a linear scaling factor to be discussed below. The interaction energy can be either negative or positive, but in most cases it contributes to decreasing the free energy of the charged group in the protein. The transfer energy generally is positive because the protein interior is less hydrophilic than water and the energy required to desolvate is not completely compensated by subsequent resolvation of the group in the protein. Moreover, the more hydrophobic the local environment in the protein, the less desolvation energy will be compensated. For titratable groups located at the surface of the protein, both interaction and transfer energies are usually small, yielding only small pK_a shifts. This article is focused on titratable residues that are buried in the protein interior, where both energy components can be very large.

The reliable calculation of pK_a shifts that stabilize the neutral state is of great interest because this type of shift is often associated with function, e.g., Glu35 in lysozyme,[3] Asp26 in thioredoxin,[4] Asp 96 and Asp115 in bacteriorhodopsin,[28] Glu 134 in rhodopsin,[29] and its conserved sequence analog in other G-protein coupled receptors.[30] From this partial list it is clear that the ability to reliably calculate the pK_a of deeply buried titratable groups is of considerable practical importance in understanding structure-function relationships. This is especially true for the trans-membrane proteins because of the difficulty of measuring the pK_a experimentally in these systems.

The quantities, w^{int} and Δw^{tr}, provide two different mechanisms that can shift pK_a values: A large w^{int} can be achieved simply by the appropriate arrangement of charges around the titratable group, although this may not necessarily lead to a particularly stable arrangement for the protein as a whole. In contrast, large, positive transfer energies can be realized by the appropriate architectural arrangement of hydrophobic groups in the microenvironment around the titratable group in the protein. In such cases the transfer energy is positive and therefore favors the uncharged state of the TR. To capture this property correctly in pK_a calculations, it is necessary to describe the hydrophobicity of the microenvironment quantitatively.[31]

In an earlier article an approach was proposed for calculating the pK_a of protonatable residues in proteins based on screened Coulomb potentials (SCPs) and a variational technique for distributing the titration charge on the atoms of the titratable moiety.[32] The method was essentially parameter free, using only one parameter that damped the interaction energy between atoms with separation less than the van der Waals distance. The method was of similar accuracy as those using the Poisson Boltzmann equation[33] but considerably faster. Nevertheless, both methods failed in correctly predicting the pK_a values of certain key residues such as Glu35 in lysozyme, which has a measured pK_a of 6.1,[34] but the calculated value was around 4.5.[33] Examination of the local environment around Glu35 indicated that it was much more hydrophobic than the average local environment around titratable residues, and it was hypothesized that the transfer of a charged group from water into such a hydrophobic microenvironment would substantially increase the energy penalty.

To quantitatively characterize the microenvironment, it was proposed to use the Hydrophobic Fragmental Constants developed by Rekker.[35–38] As described in detail in Ref. 31 the improved approach uses the degree of burial of the given titratable moiety, and the hydrophobicity of its microenvironment to modulate both the interaction (w^{int}) and transfer (Δw^{tr}) contributions to the electrostatic free energy. Application of the modified approach to lysozyme, yielded a pK_a value of Glu35 in good agreement with experiment; the pK_a values of the other TRs also were in good agreement with the measured quantities with an overall RMSD (root mean square difference between calculated and experimental pK_a values) of 0.5.[31]

In this article the treatment of very hydrophobic microenvironments for calculating pK_a values is extended. To further calibrate the SCP-based approach for such cases three mutants of staphylococcal nuclease (SNase) were used, where deeply buried hydrophobic residues have been replaced by TRs. Subsequently, the method was applied to calculate the pK_a value of another buried TR in SNase that was not used in the calibration, and the pK_a value of a deeply buried, active site aspartate at position 300 in pea seedling amine oxidase (PSAO). PSAO is a very large, copper containing, dimeric protein consisting of 1284 residues, which belongs to a general class of catalysts that carry out oxidative deamination of primary amines to aldehydes.[39–41] The Asp at position 300 has been proposed

to play the role of a general base in the reductive step of the PSAO catalytic cycle.

MATERIALS AND METHODS

Electrostatic calculation

Evaluation of the quantities w_A^{int} and Δw_A^{tr} was described in detail previously[31] and is based on using an SCP of the form

$$\Phi(\mathbf{r}) = \sum_j \frac{q_j}{D(r_j) r_j} \tag{3}$$

where $r_j = |\mathbf{r} - \mathbf{r}_j|$, q_j is the charge on atom j located at $\mathbf{r}_j$ and $D(r)$ is the screening function, which is known to be of sigmoidal form.[42–44] It can be represented analytically by the differential equation

$$dD(r)/dr = \lambda\,(D_o + D)\,(D_s - D) \tag{4}$$

with solutions

$$D(r) = B/[1 + k\,exp(-\lambda B r)] - D_o \tag{5}$$

where $B = D_s + D_o$, k is a constant of integration, D_o and λ are parameters, and D_s is the dielectric constant of water with a value of 78.4. It is convenient to set $D(0) = 1$ by taking $k = (D_s - 1)/(D_o + 1)$. Then the two parameters D_o and λ define the explicit form of the solutions of Eq. (4).

To carry out the calculations a variational approach was developed to optimally distribute the ionization charge over the atoms of the titratable moiety as has been described.[31,32] Briefly, the partial charge on an atom, a, in group A is defined as

$$q_a = (1 - \theta_A)\, q_a^n + f_a\, q_a^o \tag{6}$$

q_a^n is the partial charge from the neutral group, θ_A is the fraction of A in the charged state, q_a^o is a fixed initial partial charge ($\neq 0$ for the atoms of titratable groups and 0 otherwise), and the f_a are scaling factors that are subject to variation to determine a stationary point of $w = \sum w_A = \sum w_A^{\text{int}} + \alpha_A \Delta w_A^{\text{tr}}$, where $w_A^{\text{int}} = \sum w_a^{\text{int}}$,

$$w_a^{\text{int}} = \frac{1}{2} f_a\, q_a^o\, \Phi_a(\mathbf{r}_a) \tag{7}$$

and Δw^{tr} will be defined below. Because the energy depends on how the ionization charge is distributed, this approach leads to a relationship between the ionization charge distribution and the energy that must be satisfied. It is of the form $d = f(w(d))$, where d represents the charge distribution defined by all the charges q_a of Eq. (6), $w(d)$ is the energy term, and $f(x)$ is the expression found from the variational procedure, i.e., requiring that $\delta w = 0$ with constraints that require the total charge on group A, q_A, to remain constant at a given pH. These equations are solved iteratively starting from some initial guess for d, d^o, and convergence is achieved when $d^n - d^{n-1}$ is less than a preselected threshold. The pH dependence of the equilibrium charge state is coupled to the variational equations using the Henderson-Hasselbach equation, which, because of the self-consistency condition, is corrected to all orders. In this way the need for explicitly enumerating 2^N microstates[27,45,46] is avoided, but as a consequence the net charge on a TR can have noninteger values. From the convergence criterion ($q_A = \sum_a q_a^o f_a = Z_A \theta_A$, where Z_A is the formal charge on $TR\,A$),[31] it is seen that the net charge is proportional to the calculated concentration of the charged species at the given pH. It is also noted that the variational condition used here is exact, but because it is applied to the distribution of the titration charge only, all nonelectrostatic terms are constant.

Microenvironments

It has long been recognized that the inhomogeneity of proteins is an inherent characteristic of these macromolecules, and a key determinant of their properties. Nevertheless, the development of quantitative descriptors for characterizing inhomogeneity has been slow. Early work in this direction was published by Ponnuswamy[47] who developed a scheme for characterizing the local environments around each amino acid residue. The work provided early evidence of the lack of correlation between extent of burial and other properties. Another approach to define descriptors of local environment was developed by D. Eisenberg and collaborators for identifying structural homology in cases of little or no sequence homology.[48] The method was recently applied to human bactericidal/permeability-increasing protein.[49]

In the above approaches characterization of the microenvironment was based on the hydrophobicity of the whole residue or side chain.[50] As discussed in Ref. 31, because the titration charge is usually placed on a small group of atoms comprising a subset of the side chains of the TRs, the whole residue hydrophobicity scales were not suitable. In addition, the hydrophobicity of many side chains is not uniform over their entire extent; many have both hydrophobic and polar or charged regions that are not well represented by a single quantity. Another important consideration was the generality of the scale: extension of a scale to include nucleic acids, ligands, coenzymes and other biologically important functionalities would be difficult and could lead to inconsistencies, starting from a scale based only on amino acid residues. All these considerations suggested that an atom or fragment based hydrophobicity scale was most appropriate for quantifying the microenvironments around titratable groups.

Several fragment based[35,51,52] and one atom based[53] hydrophobicity scales have been proposed. Previously,[31] and in the present work, the Rekker Scale is used to quantify the microenvironments. It was the first fragmental scale developed and is based on assigning hydrophobicity values and correction factors to small functional fragments. The Rekker scale as well as the other fragmental scales were all constructed to calculate water/octanol partition coefficients (log P) for potential drug candidates. Recent analysis indicates that the Rekker scale is one of the most reliable for calculating log P values.[54] Moreover, it was parametrized using a very large set of organic molecules including amino acid residue analogues. Therefore, it provides a uniform set of parameters applicable to

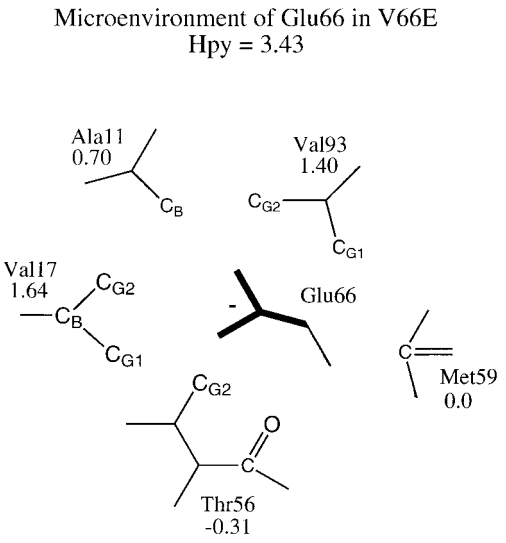

Fig. 1. Schematic representation of the microenvironment around Glu66 in the V66E mutant of SNase. The individual residue contributions to the total hydrophobicity are given under the residue's three letter code. Only atoms that are within 4.25 Å of any atom of the titratable moiety of Glu66 (shown in bold) are labled.

the many organic functionalities, beside amino acid residues, that are biologically active.

The detailed method used to quantify the microenvironment has been reported.[31] The microenvironment is defined as the volume swept out by spheres of radius 4.25 Å centered on each nonhydrogen atom belonging to the given group. Any atom (or fragment) of other residues that lies within any of these spheres contributes the value of its Rekker hydrophobic fragmental constant to the total hydrophobicity/hydrophilicity (Hpy) of that microenvironment (see Fig. 1). In analogy to the way log P is calculated from the fragmental constants, Hpy is expressed as

$$Hpy_A = \sum_{a}^{N_A} \sum_{Bb} d_b \, RFHC_b \; (r_{ab} \leq 4.25 \text{ Å}) \quad (\text{B} \neq \text{A}) \qquad (8)$$

where $RFHC_b$ is the contribution of atom b in group B to the fragment's fragmental hydrophobic constant, N_A is the number of atoms in group A and $d_b = 1$ if atom b has not been counted, or 0, if it has been counted, to ensure that each atom in the microenvironment is counted only once. It is noted that Hpy quantitatively characterizes the contribution of the protein to the microenvironment, but it does not contain any information pertaining to the degree of burial of the group or the contribution of accessible solvent to the hydrophobicity of the the group. To incorporate these descriptors into the quantitative description of the microenvironment, two additional quantities are defined, namely

$$THpy_A = BF_A \, Hpy_A + (1 - BF_A) \, Hpy_A^o \qquad (9)$$

and

$$rHpy_A = THpy_A / Hpy_A^o \qquad (10)$$

where BF_A is the buried fraction of group A (calculated from the average of the BFs of its constituent atoms), and Hpy_A^o is the hydrophilicity of the microenvironment when the group is completely immersed in solvent.[31] The quantity THpy calculated in Eq. (9) is the total hydrophobicity of the microenvironment consisting of the protein contribution and the solvent contribution weighted by the buried fraction (BF_A) and solvent exposed fraction ($1 - BF_A$), respectively.

A drawback of the quantities Hpy and THpy is that they are not normalized and therefore not suitable to characterize the relative hydrophobicities of different groups in a given microenvironment. In contrast the fractional hydrophobicity, rHpy, defined in Eq. (10), normalizes THpy relative to the hydrophilicity of the microenvironment of the group completely surrounded by solvent. Because of this it is a local property index (LPI) that is suitable for characterizing the relative hydrophobicities of fragments in given microenvironments. In the Rekker scale, hydrophilic fragments have negative fragmental constants, whereas positive values indicate hydrophobic fragments, so that Hpy can be positive or negative. In water the microenvironment is negative for all titratable fragments.[31] rHpy can therefore, be positive or negative; values greater than one would indicate microenvironments that are more hydrophilic that water. Values < 0.25 are typical for fairly hydrophobic microenvironments whereas values <0 indicate extremely hydrophobic environments. These ideas are illustrated in Figure 1, which presents a schematic diagram of the microenvironment around one of the mutants of SNase used in this study. Additionally, Figure 1 shows how the conformations of Thr56 and Met59 position most of the hydrophilic fragments outside the microenvironment further enhancing its hydrophobicity. The value of rHpy is -0.26, indicating an extremely hydrophobic microenvironment for this titratable group.

In cases where a polar or charged group is deeply buried in a hydrophobic local environment, it is quite likely that water molecules will penetrate into the region to help stabilize the polar group.[17] Although the presence of water in such regions probably is quite general, they are not always crystallographically resolved. These considerations suggest that the most consistent way to proceed is to exclude the explicit representation of these waters and to account for them as part of the bulk solvent. A pK_a calculation including explicit waters was recently reported that studied specificity and catalysis of Uracyl DNA Glycosylase.[55] In that study the pK_a were calculated as averages from pK_a values computed from coordinate sets in a Molecular Dynamics trajectory. It is noteworthy that the pK_a calculation itself is fast enough that it can be repeated many times from the coordinate sets in a trajectory to obtain a statistically valid mean.

Calculation of the Transfer Energy

It was shown earlier[32,56] that the transfer energy could be evaluated from the integral form of the Born equation and has the form

$$\Delta w_a^{tr} = (f_a q_a^o)^2 \frac{1}{2}\left\{\frac{1}{D_p(R_a^p)R_a^b} - \frac{1}{D_s(R_a^s)R_a^s}\right\}(BF)_a \quad (11)$$

where R_a^p, D_p, and R_a^s, D_s are effective Born radii and screening functions in the protein and solvent, respectively, and BF_a is the buried fraction of atom a averaged over the atoms of the titratable group. In the calculations carried out earlier[31] as well as in this work, the Born approximation has been used so that $R_a \equiv R_a^p = R_a^s$ and R_a is evaluated from solvation free energies as described previously.[32] Although the Born radii, R_a, evaluated in this way were sufficient for most cases where the microenvironments around titratable groups do not deviate too far from their average values (see results, below) they were unable to account for transfers to highly hydrophobic microenvironments.[32] This should not be surprising, because such microenvironments are very far from the hydrophilic microenvironment that characterizes a titratable group in water and on which the determination of the R_a was based. Recently a parameter free model was proposed for determining effective Born radii for use in a general SCP based implicit solvent model.[57] This approach is well suited for incorporation of the modulating effects of specific microenvironments on the effective Born radii, and the development of a suitable algorithm is currently in progress.

For a given atom a, its characteristic Born radius in a protein, R_a^p, will decrease in a hydrophobic microenvironment. This occurs because hydrophobic microenvironments are characterized by the presence of carbon atoms, whereas hydrophilic microenvironments by N or O atoms. However, carbon has a larger van der Waals radius than either N or O and accounting for this in the calculation of R_a^p will cause it to decrease (see also Refs. 43, 58, and 59). From this it follows that the first term in Eq. (11) will be larger for hydrophobic microenvironments, leading to an increase in the value of Δw^{tr}. To model this effect in the case of E35 in lysozyme, and other systems, a linear scaling of the transfer energy was proposed[31] to calculate the pK_a of TRs in these hydrophobic microenvironments. In spite of the approximate nature of this procedure it gave reasonable results for Glu35 in lysozyme and made possible an initial assessment of the role of the transfer energy in the SCP-based approach. To further extend that study, we will continue to use this scaling approach, but it will be applied to additional systems with titratable residues buried in extremely hydrophobic microenvironments.

Computational Details

All calculations use the same protocol as reported previously[31] except as otherwise noted. The program was modified to calculate the solvent accessible surface areas internally instead of using CHARMM[60] by incorporating part of the GEPOL93 package.[61] The coordinates are prepared as before by using the HBUILD command in CHARMM to add hydrogens. No subsequent minimization is carried out. The reference pK_a values used were N-term 7.5, C-term 3.8, His 6.3, Glu 4.4, Asp 4.0, Tyr 10.0, Lys 10.4, and Arg 12.0. Partial charges are taken from the PAR19 force field[60] except the neutral forms of the titratable moieties that are taken from PAR22[62,63]; the titratable groups are the same as defined in PAR19.

Preparation of PSAO required some special considerations: The crystal structure[64] was completed by adding the missing atoms to the terminal cysteine residues and building the hydrogens as above. All crystallographic water molecules were removed with the exception of those that are bound to the Mn^{2+} and Cu^{2+} ions. These waters, however, are not close to the residues of interest, and their presence should not affect the pK_a values of the active site groups. Six sugar residues bound to Asn-131, Asn-334, and Asn-558 were also excluded. Because these glycosylation sites are located on the surface of the enzyme, the deglycosylation is not expected to influence the structure. Two disordered residues have been observed in the crystal structure: His 420 and 840. As multiple positions can be handled only in separate calculations, in the present work only positions A were used with full occupancy.

The charge distribution for the Topa-quinone (TPQ) cofactor was calculated using 6-31G* basis sets and the charges were obtained by fitting to the electrostatic potentials by a Merz-Kollman scheme, implemented in the Gaussian program.[65] TPQ was truncated at Cβ and completed with a hydrogen, which was merged with the charge of the Cβ atom. Charge distributions were determined for two TPQ models of different size but yielded only minor differences in the charges of the ring atoms. Hence, TPQ was parametrized based on the charges calculated for the above model. The degree of solvent accessibility for all groups in PSAO was calculated by CHARMM.[60] The Rekker coefficients for TPQ were derived from those of tyrosine[31]; the data are available upon request.

RESULTS AND DISCUSSION

Microenvironments around Titratable Groups

The microenvironments of the titratable groups in a set of seven proteins studied earlier[31] were in most cases found to be quite hydrophilic, although in all cases less hydrophilic than water. The proteins studied in this work follow the same trend: In PHS, one of the hyperstable variants of SNase used to measure the energetics of ionization of TRs in hydrophobic environments,[16] about 19% of the TRs are more than 70% buried and the Hpy values of 31% of the TRs are greater than zero. However, only the THpy value of Asp77 is larger than 0 and only for this residue is $\alpha > 1$. In PSAO the results are even more remarkable. Each monomer in the dimer comprises 642 residues of which 167 (including the termini) are titratable. In the dimer almost half of the TRs are more than 70% buried, yet only 20% of them have Hpy values > 0, and only 14 have THpy > 0.

To obtain further insight in the role of the microenvironments in the structure and function of proteins, a data base of 204 monomeric proteins was constructed from a list of known protein structure with less than 25% sequence identity between them.[66] The proteins in the database range from 31 to 839 residues in length. The mean values and standard deviations of the microenvironment descrip-

TABLE I. Average Values of the Microenvironment Properties for Each Type of Titratable Residue[†]

Res (No)	$\overline{BF}$	$\overline{Hpy}$	$\overline{THpy}$	$\overline{rHpy}$
Tyr (1628)	0.73 (0.27)	−0.06 (1.77)	−2.25 (2.66)	0.28 (0.33)
His (932)	0.71 (0.23)	−3.04 (2.50)	−10.1 (5.81)	0.37 (0.21)
Asp (2461)	0.59 (0.25)	−2.64 (1.97)	−8.47 (3.53)	0.51 (0.21)
Arg (1912)	0.57 (0.25)	−1.59 (2.18)	−13.4 (6.51)	0.47 (0.22)
Glu (2441)	0.52 (0.25)	−1.30 (1.83)	−8.69 (3.87)	0.53 (0.24)
Lys (2413)	0.40 (0.24)	−1.04 (1.42)	−12.1 (4.13)	0.63 (0.21)

[†]Averages calculated from a 204 protein data set; see text. Values in parentheses in columns 2–5 are the standard deviations.

TABLE II. Anomalous Hydrophobic Microenvironments around Buried Titratable Groups in Lysozyme and Mutants of SNase

Protein[a]	BF	Hpy	THpy	rHpy
Lysozyme E35	0.87	1.25	−0.59	0.05
PHS/V66D	0.98	0.16	−0.13	0.01
PHS/V66E	1.00	3.43	3.39	−0.26
Δ+PHS/V66K	1.00	3.67	3.67	−0.32
Δ+PHS/I92E	0.99	5.68	5.40	−0.42

[a]PHS = SNase mutant with P117G, H124L, and S128A substitutions. Δ+PHS = PHS with additional substitutions G50F and V51N, and a 44–49 deletion.

tors around the titratable groups in this data base have been calculated for each type of TR and are given in Table I. It is apparent that in terms of the buried fraction, the TRs cluster into three groups: i) Tyr and His; ii) Asp, Arg and Glu; and iii) Lys. Tyr and His are the most buried TRs, because stabilization of their aromatic moieties requires exclusion of water. Note also that negative values of rHpy (i.e., extremely hydrophobic microenvironments) are within one and two standard deviations of the average value for Tyr and His, respectively. However, for both these residues hydrophobic microenvironments will shift their pK_a to values further away from the physiological pH range and stabilize the neutral state. These two residues can be shifted into the appropriate pH range by favorable interactions with polar or other charged groups and forming hydrogen bonds. For the remaining TRs the effect of a hydrophobic microenvironment is to shift their pK_a closer to physiological pH.

The value of rHpy for Asp, Glu, and Arg have to be shifted by less than 2.5 standard deviations to put their microenvironments in the very hydrophobic range that has the potential to generate large pK_a shifts. However, Arg would require a pK_a shift of about 5 units to put it in the relevant pH range, whereas Asp and Glu require shifts of only 2–3 pK units. From the mean value of BF for lysine it appears that this residue is most often found on the surface in most proteins. The mean value of rHpy is substantially larger than for any other TR, which reflects the increased mean solvent exposure of Lys. Moreover, the value of rHpy would have to decrease by more than 3 standard deviations for the microenvironment to become substantially hydrophobic. Although the authors are not aware of any quantitative assessment of the relative frequency that the pK_a of TRs are shifted into the physiological range and are directly involved in enzymatic catalysis, the data in Table I suggest that Asp and Glu would most frequently act as proton donors or acceptors in enzymatic reactions, and lysine less often. Arginine would require nearly 7 kcal/mol for its pK_a to shift to the appropriate region.

Calibration of the Transfer Energy Scaling with Buried Groups in SNase

The SNase mutants, V66D, V66E, V66K, and I92E, provide an opportunity to extend the analysis of the effect of hydrophobic microenvironments on the pK_a of titratable residues. In the structures of these mutants the ionizable side chains at positions 66 or 92 can be seen in their entirety, buried in one of the most highly hydrophobic regions in the interior of SNase.[15] It has been demonstrated that Lys-66 and Glu-66 remain buried under pH conditions where the titratable moieties are ionized. Buried water molecules are associated with Glu-66[16] and Glu-92. No buried waters have ever been detected in structures with Lys-66, and the pattern of hydration of Asp-66 is temperature sensitive: buried water molecules are visible in the structure obtained under cryogenic conditions (−170°C) but invisible at room temperature (Karp, Stahley, Gittis, Lattman, and Garcia-Moreno, in preparation).

The quantitative descriptors of the microenvironment around E35 in lysozyme and the four mutants of SNase are listed in Table II. Comparison of these values with the averages given in Table I confirms that all these microenvironments are unusual, with all descriptors deviating more than two standard deviations from their mean values. Another way to understand this is by noting that the reciprocal of the mean value of rHpy yields an approximate measure of the change in hydrophobicity in transferring the titratable group from water into the protein. From Table I this change ranges from about 3.5 (for tyrosine) to 1.5 (for lysine). Clearly the change in hydrophobicity is very much larger for the groups given in Table II. It is seen that the microenvironment of I92 is the most hydrophobic. Finally, it should be noted that even a small fraction exposed to solvent has a strong effect on the microenvironment as seen for E35 of lysozyme. The value of Hpy is smaller for SNase V66D, but because its BF is greater, rHpy is smaller than in E35 of lysozyme.

To determine appropriate factors for scaling the transfer energy in the different microenvironments, the four systems, lysozyme E35, and the V66D, V66E, and V66K mutants of SNase were considered. The crystallographic structure of the I92E mutant was completed after the scaling factors had been determined based on the data for E35 and the buried ionizable residues at position 66, affording an independent test of the parametrization based on the other mutants of V66 in SNase and lysozyme. From the experimental pK_a values of the four TRs and their rHpy values, microenvironments with rHpy $\leq$ 0.1 were assigned linear scaling factors as follows: for 0.02 $\leq$ rHpy $\leq$ 0.100, α = 2; and for rHpy $\leq$ 0.02, α = 3. In all

TABLE III. pK_a Values of Titratable Groups in Anomalous Hydrophobic Environments

Protein[a]	α	pK_a[b]	Exp pK_a	Error	w^{int} (Kcal/mol)	$\alpha\Delta w^{tr}$ (Kcal/mol)
Lysozyme E35	2.0	6.17 (6.8)	6.2	−0.03 (0.7)	−0.97	3.40
PHS/V66D	3.0	8.47 (7.8)	8.7	−0.23 (−0.9)	0.60	5.54
PHS/V66E	3.0	8.92 (8.2)	8.8	0.12 (−0.6)	0.31	6.00
Δ+PHS/V66K	3.0	5.99 (6.8)	5.7	0.29 (1.1)	−0.28	6.32
Δ+PHS/I92E	3.0	8.67	8.8	−0.13	0.04	5.61

[a]See footnote a, Table II, for nomenclature.
[b]Numbers in parentheses are pK_a values and errors calculated with $\alpha = 2.5$.

other cases, i.e., when rHpy > 0.1, the scale factor is one. These values of α and the threshold values were determined from roughly fitting to the four pK_a values given above, but a more accurate fit was not carried out because of lack of sufficient data. Instead, the reliability of the assignment was tested by application to additional structures. All other parameters are identical to those used previously.[31]

Inspection of the protein data base used for Table I indicates that the smallest value of BF for which the threshold value of rHpy = 0.10 is reached is about 0.75, in agreement with earlier studies. There it was found that when BF ≤ 0.7, the effects of solvent on the microenvironment rapidly become dominant. This happens because the solvent's contribution to the Thpy is negative and large in magnitude (it is about −13 for an Asp or Glu fully immersed in water). Therefore, as shown by lysozyme, even a small degree of solvent exposure rapidly decreases the hydrophobicity of the microenvironment. It illustrates that pK_a changes cannot be predicted only on the basis of BF data or calculating electrostatic interactions with other ionizable groups.

The pK_a values calculated for the buried TRs in SNase are presented in Table III, and the results show that for the four values used in calibrating α and for the test case, I92E, the agreement between calculated and experimental pK_a values is excellent. The values of the energy components show that in all cases the transfer energy is the dominant contribution, but for E35 the interaction energy is almost −1 kcal/mol contributing to the much smaller pK_a shift for that case; in contrast the interaction energy of V66D contributes about 0.4 pK_a units to the total shift.

To explore the dependence of the calculated pK_a values on the scaling factors, they were also calculated for $\alpha = 2.5$. It is seen that a change in α of one-half unit changes the pK_a value by about 0.8 units. This sensitivity of the pK_a to the value of the linear scaling factor shows that in spite of its approximate nature, it is properly modeling the sensitivity of the transfer energy to small changes in the value of the characteristic Born radius, R_α^p. This sensitivity arises because the Born radii are small (<2.5 Å). Thus, $D(R_\alpha^p)$ is small and highly nonlinear,[31] so that the response of the first term in brackets in Eq. (11) to small changes in R_α^p will be large. The nonlinear nature of the response of a TR to a hydrophobic microenvironment is also shown by the large pK_a shift of V66D: Its microenvironment is less hydrophobic than the microenvironments of the other SNase mutants, but the transfer energy is almost as large as for the other mutants. Moreover, these results clearly show that Born radii calculated from solvation free energies do not capture correctly the self energy of charges transferred from water to highly hydrophobic microenvironments.

TABLE IV. pK_a Values of Histidines in SNase[†]

His	exp pK_a	calc pK_a	Error	BF	Hpy	rHpy
8	6.53	6.18	−0.35	0.097	−1.56	0.91
46	5.90	5.34	−0.56	0.746	−2.98	0.37
121	5.31	5.85	0.54	0.766	0.71	0.20

[†]Experimental values and calculations of the PHS mutant of SNase. See Table II for nomenclature.

Histidine pK_a values in SNase

To demonstrate that the local treatment of the TRs in hydrophobic microenvironments does not adversely affect the reliability of the calculated values of pK_a in microenvironments that are closer to the mean values indicated in Table I, the pK_a values of histidines in PHS nuclease were estimated. The results are reported in Table IV. His 8 is completely exposed to solvent, and both the interaction and self-energy terms are small, so that the calculated pK_a is close to the reference value. Note that the microenvironments of His46 and His121 are close to the average values for histidines (see Table I). In spite of the BF of these two residues being >0.7, the values of rHpy are larger than the threshold value of 0.10 for which α is increased to a value >1. The interaction energies of both titratable moieties are small, but because of the fairly hydrophobic microenvironments, the pK_a values are depressed below the reference value of 6.3. For all three histidines the calculated pK_a values are in reasonable agreement with the measured values.

Pea Seedling Amine Oxidase (PSAO)

Calculation of the pK_a values of all ionizable residues were carried out in the pH range of 5–10, in steps of 1 pH unit. More than half of the TRs are bases [Lys (76), Arg (54), and His (50)] that are either expected to titrate at a higher pH than Asp 300 or TPQ (Lys and Arg) or are not expected to affect the pK_a of the active site groups. Considerable CPU time can be saved by fixing the ionization states of these residues (positive charge for Lys and Arg and neutral state for His). However, because of the variational procedure used to calculate the pK_a by assign-

TABLE V. Microenvironments of Asp 300 and TPQ in PSAO

	BF	α	Hpy	THpy	rHpy
Asp-300 (A)	1.000	3.00	4.25	4.25	−0.31
Asp-300 (B)	1.000	3.00	1.11	1.11	−0.08
TPQ (A)	0.984	1.00	−1.87	−2.13	0.11
TPQ (B)	0.999	1.00	−2.41	−2.42	0.13

ing the titratable charge in an optimal way over the atoms of the protonatable moieties,[31] fixing them in a particular charge state with fixed charge assignments can affect the value of the pK_a of the residues being titrated. To study this effect four different titration schemes were used for the basic residues: (1) all Arg, Lys and His sidechains were titrated; (2) all Lys and Arg were titrated as well as the His in the proximity of TPQ: (His-442 and His-444); (3) all Lys and Arg were titrated, and all His residues were excluded from the titration; (4) all Lys, Arg and His were excluded from the titration. Two additional titration schemes were designed to assess the effect of titrating the negatively charged TPQ cofactor on the pK_a of Asp-300. Because schemes 1–4 showed that titration of His residues exerts only a minor effect on the pK_a of Asp (see below), but their inclusion slows down the convergence considerably, the ionization states of all His were kept fixed in these calculations. We only switched off (scheme 5) and on (scheme 6) the titration of Lys and Arg residues, while TPQ was titrated in both cases. A further benefit of reducing the number of groups to titrate is that it improves the convergence of the calculations. It is also worthwhile to note that this huge system required at least 2000 steps to converge at each pH (for scheme 6), which required a total of 8 CPU hours on a SGI R10000 processor.

The microenvironment parameters around the titratable moieties of Asp-300 and TPQ in both subunits of PSAO are listed in Table V. The values show that the local environment around Asp-300 (A and B) are in the same range as in the SNase mutants (Table II), whereas around TPQ they are much less hydrophobic, e.g., more like His 46 and 121 in SNase (Table IV). Because both the aspartates and the TPQs are completely buried, Table V provides another example that proteins are capable of creating microenvironments with a wide range of properties around functionally important groups. Asp-300 is located at the bottom of a channel along which the substrate travels to the active site. One side of the channel is formed by mostly hydrophobic residues that protect the active site from water, which is essential for radical formation in the oxidative part of the reaction. The difference between the rHpy values of Asp-300 in the two subunits is due to the variability in the conformation of the negatively charged TPQ cofactor in the two monomers and to the normal fluctuations of the protein. The difference in the rHpy values results in 0.15 pH unit difference in the pK_a's of Asp-300 between the two subunits when TPQ is present, whereas it diminishes when the TPQ is mutated to Gly.

The pK_a values calculated for Asp-300 in subunit A with the different titration schemes are summarized in Table VI (note that the results for subunit B are similar). The results indicate that the calculated pK_a of Asp-A300 is fairly insensitive to which basic residues are titrated and varies between 8.7 and 9.1, with the main difference coming from the way TPQ is treated. The reason for this can be seen from the values of w^{int} and $\alpha\Delta w^{tr}$ values presented in Table VI for the various titration schemes. The predominant contribution comes from the transfer energy and is practically constant. Similarly, the interaction energy shows little variability to changes in which basic residues are included or excluded from the titration, but is somewhat more responsive to titration of TPQ that decreases the pK_a by almost 0.3 pK units (schemes 5 and 6 in Table VI). Titration scheme 6 includes all residues that were shown to affect the pK_a of Asp 300. It is also the scheme that yields a pK_a value closest to the experimental result obtained from kinetic data that indicates the reaction requires a TR at the active site with a pK_a of 8.3 ± 0.1 (DiPaolo and Scarpa, private communication), which should act as a general base.

TPQ is an essential cofactor for the deamination reaction. This negatively charged residue is located within hydrogen bonding distance of Asp-300. The electrostatic interaction energy between the carboxyl group of Asp-300 and the TPQ side chain is 0.8 kcal/mol at pH = 8.7, corresponding to a pK_a increase of 0.5 units. As seen from Table VI other contributions to the interaction energy essentially cancel.

CONCLUSIONS

In this article it has been shown that the approach for calculating pK_a based on screened Coulomb potentials can be reliably extended to titratable residues in extremely hydrophobic local environments that produce very large pK_a shifts. The key element that makes this possible is the quantitative characterization of the microenvironments by their hydrophobicity or hydrophilicity. An analysis of the average microenvironment around titratable groups indicated that they are fairly hydrophilic, making it straightforward to identify unusually hydrophobic microenvironments. This approach then allows such cases to be treated locally without affecting the treatment of the residues in more hydrophilic microenvironments, so that both can be calculated with reasonable accuracy and in a self-consistent manner within a single calculation. This is in contrast to continuum methods that treat the protein as a homogeneous system. In those approaches one can treat the residues in microenvironments such as those that were found on average for TRs by using a fairly large value for the dielectric screening, but then the shifts in pK_a values of TRs buried in hydrophobic environments are underestimated. Alternatively one can treat the latter by using a smaller screening factor, but then the pK_a shifts of the former will be grossly exaggerated.[33,67] The results of these studies clearly confirm the fundamental observation that proteins are extremely anisotropic systems, which must be taken into account for a proper treatment of electrostatic effects. This conclusion has long been argued

TABLE VI. pK_a Values and Energetics of Asp-A300 with Various Titration Schemes

Titr. Schm.	Arg, Lys Titrated[a]	His Titrated[a]	TPQ Titrated[a]	pK_a Asp-A300	w^{int} (Kcal/mol)	$\alpha\Delta w^{tr}$ (Kcal/mol)
1.	+	+	−	8.94	1.13	5.72
2.	+	+[b]	−	8.93	1.13	5.73
3.	+	−	−	8.92	1.11	5.75
4.	−	−	−	9.06	1.29	5.66
5.	−	−	+	8.82	0.95	5.67
6.	+	−	+	8.69	0.79	5.67
exp[c]				8.3 ± 0.1		

[a]+, groups are titrated; −, groups with fixed unit charge.
[b]Only His in the proximity of TPQ is titrated (His-442,His-444).
[c]DiPaolo and Scarpa, private communication.

by Warshel and his collaborators,[17,19] but is often sacrificed for the sake of computational simplicity.

Further modification of the method will focus on replacing the current linear scaling approach with the parameter free approach.[68] Finally, it is noted that as more data for TRs in deeply buried, hydrophobic microenvironments becomes available, it will be possible to further refine the parametrization.

ACKNOWLEDGMENT

The authors thank Dr. Pascual-Ahuir for allowing us to use GEPOL93. Computational support was provided by the Pittsburgh Supercomputer Center (sponsored by the National Science Foundation), the Cornell National Supercomputer Facility, the Advanced Scientific Computing Laboratory at the Frederick Cancer Research Facility of the National Cancer Institute (Laboratory of Mathematical Biology), and the Computer Center of the Mount Sinai School of Medicine. The authors also acknowledge access to the computer facilities at the Institute of Computational Biomedicine (ICB) of the Mount Sinai Medical Center.

REFERENCES

1. Fersht AR. Conformational equilibria in alpha-chymotrypsin and delta-chymotrypsin—energetics and importance of salt bridge. J Mol Biol 1972;64:497–509.
2. Lewis SD, Johnson FA, and Shafer JA. Effect of Cysteine-25 on the Ionization of histidine-159 in papain as determined by proton nuclear magnetic-resonance spectroscopy—evidence for a His-159-Cys-25 ion-pair and its possible role in catalysis. Biochemistry 1981;20:48–51.
3. Bartik K, Redfield C, Dobson CM. Measurement of the individual pK_a values of acidic residues of hen and turkey lysozymes by two-dimensional NMR. Biophys J 1994;66:1180–1184.
4. Chivers PT, Prehoda KE, Volkman FB, Kim BM, Markley JL, Raines TR. Microscopic pKa value of *Enscherichia coli* thioredoxin. Biochemistry 1997;36:14985–14991.
5. Doa-pin S, Andersen DE, Dahlquist FW, Mattews BW. Structural and thermodynamic consequences of burying a charged residue within the hydrophobic core of T4 lysozyme. Biochemistry 1991;30: 11521–11529.
6. Inagaki F, Kawano Y, Shimada I, Takahashi K, Miyazawa T. Nuclear magnetic resonance study of the microenvironments of histidine residues of ribonuclease T1 and carboxymethylated ribonuclease T1. J Biochem 1981;89:1185–1195.
7. Perez-Canadillas JM, Campoa-Olivas R, Lacadena J, Martinez del Pozo A, Gavilanes JG, Santoro J, Rico M, Bruix M. Characterization of pKa values and titration shifts in the cytotoxic ribonuclease α-sarcin by NMR. Relationship between electrostatic interactions, structure, and catalytic function. Biochemistry 1998;37:15865–15876.
8. Hartman FC, Milanez S, Lee EH. Ionization constants of two active-site lysyl ε-amino groups of ribulosebiphosphate carboxylase/oxynegase. J Biol Chem 1985;260:13968–13975.
9. Gunner MR, Nicholls A, Honig B. Electrostatic potentials in Rhodopseudomonas viridis reaction centers: Implications for the driving force and directionality of electron transfer. J Phys Chem 1996;100:4277–4291.
10. Matthew JB, Weber PC, Salemme FR, Richards FM. Electrostatic orientation during electron transfer between flavodoxin and cytochrome c. Nature 1983;301:169–171.
11. Paddock ML, Feher G, Okamura MY. Pathway of proton transfer in bacterial reaction centers: further investigations on the role of Ser-L223 studied by site-directed mutagenesis. Biochemistry 1995; 34(48):15742–15750.
12. Warshel A, Chu ZT, Parson WW. Dispersed polaron simulation of electron transfer in photosynthetic reaction center. Science 1989; 246:112–116.
13. Giletto A, Pace CN. Buried, charged, non-ion paired aspartic acid 76 contributes favorably to the conformational stability of ribonuclease. Biochemistry 1999;38:13379–13384.
14. Schaller W, Robertson AD. pH, ionic strength, and temperature dependence of ionization equilibria for the carboxyl groups in turkey ovomucoid third domain. Biochemistry 1995;34:4714–4723.
15. Dwyer JJ, Gittis AG, Karp D, Lattman EE, Spencer DS, Stites WE, Garcia-Moreno EB. High apparent dielectric constants in the interior of a protein reflect water penetration. Biophys J 2000;79: 1610–1620.
16. Garcia-Moreno B, Dwyer JJ, Gittis AG, Lattman EE, Spencer DS, Stites WE. Experimental measurement of the effective dielectric in the hydrophobic core of a protein. Biophys Chem 1997;64:211–224.
17. Schutz CN, Warshel A. What are the dielectric "constants" of proteins and how to validate electrostatic models? Proteins Struct Funct Genet 2001;44:400–417.
18. Warshel A, Russell ST. Calculation of electrostatic interactions in biological systems and in solutions. Quart Rev Biophys 1984;17: 283–422.
19. Warshel A, Russell ST, Churg AK. Macroscopic models for studies of electrostatic interactions in proteins: limits and applicability. Proc Natl Acad Sci USA 1984;81:4785–4789.
20. Sham YY, Muegge I, Warshel A. The effect of protein relaxation on charge-charge interactions and dielectric constants of proteins. Biophys J 1998;74:1744–1753.
21. Sham YY, Chu ZT, Warshel A. Consistent calculations of pKa's of ionizable residues in proteins: semi-microscopic and microscopic approaches. J Phys Chem B 1997;101:4458–4472.
22. Warshel A, Papazyan A. Electrostatic effects in macromolecules: fundamental concepts and practical modeling. Curr Opin Struct Biol 1998;8:211–217.
23. Russel ST, Warshel A. Calculations of electrostatic energies in proteins. J Mol Biol 1985;185:389–404.
24. Whitten ST, Garcia-Moreno EB. pH Dependence of stability of staphylococcal nuclease: evidence of substantial electrostatic interactions in the denatured state. Biochemistry 2000;39:14292–14304.
25. Rabold A, Bauer R, Zundel G. Structurally symmetrical N + H . . . H + N bonds. The proton potential as a function of the pKa

of the N-base. FTIR results and quantum chemical calculations. J Am Chem Soc 1995;99:1889–1895.
26. Warshel A. Calculations of enzymatic reactions: calculations of pK_a, proton transfer reactions, and general acid catalysis reactions in enzymes. Biochemistry 1981;20:3167–3177.
27. Bashford D, Karplus M. pK_a's of ionizable groups in proteins: atomic detail from a continuum electrostatic model. Biochemistry 1990;29:10219–10225.
28. Gerwert K, Ganter UM, Siebert F, Hess B. Only water exposed carboxyl groups are protonated during transition to the cation free bacteriorhodopsin. FEBS Lett 1987;213:39–44.
29. Fahmy K, Sakmar TP, Siebert F. Transducin-dependent protonation of glutamic acid 134 in rhodopsin. Biochemistry 2000;39: 10607–10612.
30. Ballesteros JA, Kitanovic S, Guarnieri F, Davies P, Fromme BJ, Konvicka K, Chi L, Millar R, Davidson JS, Weinstein H, Sealfon S. Functional microdomains in G protein-coupled receptors: the conserved arginine cage motif in the gonadotropin-releasing hormone receptor. J Biol Chem 1998;273:10445–10453.
31. Mehler EL, Guarnieri F. A self-consistent, microenvironment modulated screened Coulomb potential approximation to calculate pH dependent electrostatic effects in proteins. Biophys J 1999;77:3–22.
32. Mehler EL. A self-consistent, Free energy based approximation to calculate pH dependent electrostatic effects in proteins. J Phys Chem 1996;100:16006–16018.
33. Antosiewicz J, McCammon JA, Gilson MK. Prediction of pH-dependent properties of proteins. J Mol Biol 1994;238:415–436.
34. Kesvatera T, Jonsson B, Thulin E, Linse S. Measurement and modelling of sequence-specific pKa values of lysine residues in calbindin D_{9k}. J Mol Biol 1996;259:828–839.
35. Rekker RF. The hydrophobic fragmental constant. In: Nauta WT, Rekker RF, editors. Pharmacochemistry library. Vol. 1. Amsterdam: Elsevier; 1977.
36. Rekker RF. The hydrophobic fragmental constant; an extension to a 1000 data point set. Eur J Med Chem 1979;14:479–488.
37. Rekker RF, Mannhold R. Calculation of drug lipophilicity: the hydrophobic fragmental constant approach. Weinheim: VCH; 1992.
38. Testa B, Seiler P. Steric and lipophobic components of the hydrophobic fragmental constant. Drug Res 1981;31(II):1053–1058.
39. Klinman JP, Mu D. Quinoenzymes in biology. Annu Rev Biochem 1994;63:299–344.
40. McIntire WS, Hartmann C. Copper-containing amine oxidases. In: Davidson VL, editor. In principles and applications of quinoproteins. New York: Marcell Dekker; 1993. p 97–171.
41. Knowles PF, Doodley DM. Amine oxidases. In: Sigel H, Sigel A, editors. Metal ions in biological systems. Marcel Dekker: New York. 1994. p 361–403.
42. Conway BE, Bockris JOM, Ammar IA. The dielectric constant of the solution in the diffuse and Helmholtz double layers at a charged interface in aqueous solution. Trans Faraday Soc 1951;47: 756–767.
43. Bucher M, Porter TL. Analysis of the Born model for hydration of ions. J Phys Chem 1986;90:3406–3411.
44. Ehrenson S. Continuum radial dielectric functions for ion and dipole solution systems. J Comp Chem 1989;10:77–93.
45. Bashford D, Karplus M. Multiple-site titration curves of proteins: an analysis of exact and approximate methods for their calculation. J Phys Chem 1991;95:9556–9561.
46. Gilson MK. Multiple-site titration and molecular modeling: two rapid methods for computing energies and forces for ionizable groups in proteins. Proteins: Struct Funct Genet 1993;15:266–282.
47. Ponnuswamy PK, Prabhakaran M, Manavalan P. Hydrophobic packing and spatial arrangement of amino acid residues in globular proteins. Biochim Biophys Acta 1980;623:301–316.
48. Bowie JU, Luthy R, Eisenberg D. A method to identify protein sequences that fold into a known three-dimensional structure. Science 1991;253:164–170.
49. Kleiger G, Beamer LJ, Grothe R, Mallick P, Eisenberg D. The 1.7 Å crystal structure of BPI: a study of how two dissimilar amino acid sequences can adopt the same fold. J Mol Biol 2000;299:1019–1034.
50. Cornette JL, Cease KB, Margalit H, Spouge JL, Berzofsky JA, DeLisi C. Hydrophobicity scale and computational techniques for detecting amphipathic structures in proteins. J Mol Biol 1987;195: 659–685.
51. Suzuki T, Kudo Y. Automatic log P estimation based on combined additive modeling methods. J Comp-Aided Mol Design 1990;4:155–198.
52. Leo A, Jow PYC, Silipo C, Hansch C. Calculation of hydrophobic constant (log P) from π and f-constants. J Med Chem 1975;18:865–868.
53. Ghose AK, Crippen GM. Atomic physicochemical parameters for three-dimensional structure-directed quantitative structure-activity relationships I. partition coefficients as a measure of hydrophobicity. J Comp Chem 1986;7:565–577.
54. Mannhold R, Rekker RF, Sonntag C, ter Laak AM, Dross K, Polymeropouos EE. Comparative evaluation of the predictive power of calculation procedures for molecular lipophilicity. J Pharm Sci 1995;84:1410–1419.
55. Luo N, Mehler E, Osman R. Specificity and catalysis of uracil DNA glycosylase. A molecular dynamics study of reactant and product complexes with DNA. Biochemistry 1999;38:9209–9220.
56. Guarnieri F, Schmidt AB, Mehler EL. A screened Coulomb potential based implicit solvent model: formulation and parameter development. Int J Quantum Chem 1998;69:57–64.
57. Hassan SA, Guarnieri F, Mehler EL. A general treatment of solvent effects based on screened Coulomb potentials. J Phys Chem B 2000;104:6478–6489.
58. Latimer WM, Rodebush WH. Polarity and ionization from the standpoint of the Lewis Theory of Valence. J Am Chem Soc. 1920;42:1419–1433.
59. Rashin A, Honig B. Reevaluation of the born model of ion hydration. J Phys Chem 1985;89:5588–5593.
60. Brooks BR, Bruccoleri RE, Olafson BD, States DJ, Swaminathan S, Karplus M. CHARMM: A program for macromolecular energy, minimization and dynamics calculations. J Comput Chem 1983;4: 187–217.
61. Pascual-Ahuir JL, Silla E, Tunon I. GEPOL: an improved description of molecular surfaces. III. A new algorithm for computation of a solvent-excluding surface. J Comput chem 1994;15:1127–1138.
62. MacKerell ADJ, Bashfod D, Bellot M, Dunbrack RLJ, Field MJ, Fischer S, Gao J, Guo H, Ha S, Joseph D, Kuchnir L, Kuczera K, Lau FTK, Mattos C, Michnick S, Ngo T, Nguyen DT, Prodhom B, Roux B, Schlenkrich M, Smith J, Stote R, Straub J, Wiorkiewicz-Kuczera J, Karplus M. Self-consistent parametrization of bio molecules for molecular modeling and condensed phase simulations. Biophys J 1992;6:A143.
63. MacKerell JAD, Bashford D, Bellott M, Dunbrack RL Jr, Evanseck JD, Field MJ, Fischer S, Gao J, Guo H, Ha S, Joseph-McCarthy D, Kuchnir L, Kuczera K, Lau FTK, Mattos C, Michnick S, Ngo T, Nguyen DT, Prodhom B, Reiher IWE, Roux B, Schlenkrich M, Smith JC, Stote R, Straub J, Watanabe M, Wiorkiewicz-Kuczera J, Yin D, Karplus M. All-atom empirical potential for molecular modeling and dynamics studies of proteins. J Phys Chem B 1998;102:3586–3616.
64. Kumar VD, Dooley DM, Freeman HC, Guss JM, Harvey I, McGuirl MA, Wilce MCJ, Zubak VM. Crystal structure of eukariotic (pea seedling) copper-containing amine oxidase at 2.2 A resolution. Structure 1996;4:943–955.
65. Frisch MJ, Trucks GW, Schlegel HB, Scuseria GE, Robb MA, Cheeseman JR, Zakrzewski VG, Montgomery JAJ, Stratmann RE, Burant JC, Dapprich S, Millam JM, Daniels AD, Kudin KN, Strain MC, Farkas O, Tomasi J, Barone V, Cossi M, Cammi R, Mennucci B, Pomelli C, Adamo C, Clifford S, Ochterski J, Petersson G, Ayala PY, Cui Q, Morokuma K, Salvador P, Dannenberg JJ, Malick DK, Rabuck AD, Raghavachari K, Foresman JB, Cioslowski J, Ortiz JV, Baboul AG, Stefanov BB, Liu G, Liashenko A, Piskorz P, Komaromi I, Gomperts R, Martin RL, Fox DJ, Keith T, Al-Laham MA, Peng CY, Nanayakkara A, Challacombe M, Gill PMW, Johnson B, Chen W, Wong MW, Andres JL, Gonzalez C, Head-Gordon M, Replogle ES, Pople JA. Gaussian 98. Pittsburgh, PA: Gaussian, Inc.; 2001.
66. Hobohm U, Sander C. Enlarged representative set of protein structures. Protein Sci 1994;3:522.
67. Demchuk E, Wade RC. Improving the continuum dielectric approach to calculating pKa's of ionizable groups in proteins. J Phys Chem. 1996;100:17373–17387.
68. Hassan SA, Mehler EL. A general screened Coulomb potential based implicit solvent model: calculation of secondary structure of small peptides. Int J Quant Chem 2001;83:193–202.